Determination of salt exit velocity and its application in subsalt exploration

Yunfeng Li, Tony Huang, Nicolas Chazalnoel (CGGVeritas)

This paper was prepared for presentation during the 12th International Congress of the Brazilian Geophysical Society held in Rio de Janeiro, Brazil, August 15-18, 2011.

Abstract

In recent years, our ability to image subsalt structures has improved significantly with the availability of wide azimuth data, reverse time migration (RTM) and routine use of anisotropic imaging and tomography. In subsalt exploration, derivation of subsalt velocity, especially velocity directly below the base of salt, i.e., salt exit velocity, remains challenging because of complex salt overburden. Anomalous high BOS amplitudes can often be found, which indicate relatively strong impedance contrast at the salt-subsalt boundary. Reflectivity inversion for dirty salt is extended to derive salt exit velocity and is further combined with high resolution tomography using high-fidelity RTM 3D angle gathers to invert the sub-salt velocity model for better pressure prediction and imaging in subsalt exploration. We demonstrate the methodology with a synthetic and real WAZ data example.

Introduction

Over the past two decades, significant hydrocarbon reserves have been discovered in subsalt areas of the deepwater Gulf of Mexico. However, potential drilling hazards, such as overpressure zones directly underneath the base of salt, hinder exploration and development of hydrocarbon reservoirs. Overpressure zones refer to areas with abnormally high pore-fluid pressure in the subsurface formation. Drilling into an overpressure zone is a common cause of well blowouts, so the ability to predict such overpressure zones prior to drilling is very valuable. Overpressure zones commonly lie below thick, impermeable salt bodies and normally give lower seismic velocities compared to normal compaction trends. Lower velocity can be treated as an indicator of the subsalt overpressure (Hawkins et al., 2004). Although VSP data could provide more direct velocity measurement near wells, surface seismic data provide an economical way to extract relevant seismic velocity information away from wells, and help to identify potential drilling hazards. Here we define salt exit as the area directly underneath the base of salt (BOS) and salt exit velocity as the velocity just below the base of salt.

There are several approaches to deriving salt exit velocity. Full waveform inversion is considered the state of the art velocity inversion; however its application is limited by the lack of refracted waves underneath thick salt, as well as its high computation cost. Tomography with high fidelity RTM angle gathers provides a robust vehicle to define subsalt velocity (Xu et al., 2010), and can be extended to derive salt exit velocity. Tomography derives interval velocity for a depth interval, and its efficiency is limited by the available angles in the subsalt region. Brown and Higginbotham (2009) utilized BOS amplitude and wave equation migration (WEM) velocity focusing analysis for subsalt overpressure detection.

Alternatively, in this paper we extend the reflectivity inversion for dirty salt (Ji et al., 2010) to invert for salt exit velocity. The reflectivity is extracted from true-amplitude reverse time migration (Zhang and Sun, 2009). Salt exit velocity is inverted from a 1D equation, with compensation of transmission and illumination loss handled by 3D wave equation modeling. Then, the derived salt exit velocity from reflectivity inversion is used as a constraint for high resolution tomography using RTM 3D angle gathers to derive the subsalt velocity model. A detailed workflow is described, followed by results from a 2D synthetic dataset. The hybrid method is also applied to a wide azimuth dataset in the Gulf of Mexico. The derived subsalt velocity matches the well information very well. Both synthetic data and field data demonstrate the effectiveness of the hybrid method.

Reflectivity Inversion for Salt Exit Velocity

In recent years, seismic images and estimates of the velocity above the subsalt have improved because of the availability of wide azimuth data and advances in tomography, anisotropic imaging and RTM. Anomalous high BOS amplitudes have been noticed frequently, which indicate relatively strong impedance contrasts in the salt exit area, or the salt-subsalt boundary (Figure 1). Using two-way wave-equation shot-record modeling, we constructed a synthetic model to simulate the observation, with a zone of low subsalt velocity directly underneath the BOS (Figure 2).

Reflectivity inversion has been used to derive density with known velocity at well locations. Ji et al. (2010) used the method to obtain the velocity of sedimentary inclusion for intra-salt reflectors. The formula can further be rearranged to derive salt exit velocity, the velocity directly underneath base of salt. Because of the large impedance contrasts around salt and the complexity of the salt geometry, we need to consider factors of transmission and illumination loss. The salt exit reflection coefficient is given by

$$R_1 \times I = \frac{\rho_2 v_2 - \rho_1 v_1}{\rho_2 v_2 + \rho_1 v_1} \quad , \quad (1)$$

where R_1 is the migrated BOS amplitude, ***I*** is a transmission and illumination factor, ρ_1 is salt density, v_1 is salt velocity, v_2 is the unknown salt exit velocity, and the salt exit density (ρ_2) can be approximated by the Gardner's equation.

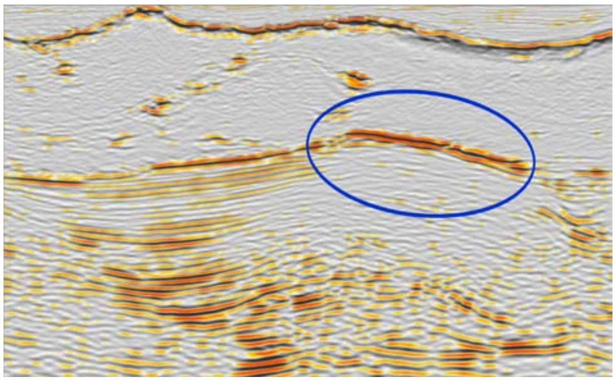

Figure 1: A typical example of anomalous high BOS amplitude in migrated data from the Gulf of Mexico.

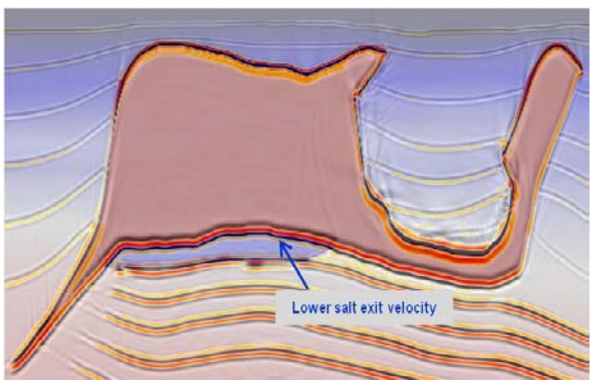

Figure 2: The salt model with lower salt exit velocity used for forward modeling, co-rendered with RTM image.

We then perform two-way wave equation modeling of the model with a normal compaction trend (v_3, known velocity), followed by reverse time migration. This gives

$$R_2 \times I = \frac{\rho_3 v_3 - \rho_1 v_1}{\rho_3 v_3 + \rho_1 v_1} \quad . \quad (2)$$

where factor *I* is approximately the same as in equation 1. By eliminating *I* from equations 1 and 2, we can obtain the unknown salt exit velocity v_2:

$$v_2 = v_1 \times \frac{(A+1) \times \rho_1}{(A-1) \times \rho_2} \quad , \quad (3)$$

Where

$$A = \frac{R_2}{R_1} \times \frac{(v_3 \rho_3 + v_1 \rho_1)}{(v_3 \rho_3 - v_1 \rho_1)} \quad . \quad (4)$$

2D Synthetic Study

A 2D synthetic dataset is used to illustrate the workflow of deriving the salt exit velocity with the reflectivity inversion followed by high-resolution tomography with RTM 3D angle gathers. The synthetic 'field' data are generated by two-way wave equation modeling of a model with a pocket of low subsalt velocity (Figure 2). The hybrid workflow is:

a) Fix supra-salt and salt geometry. Build an initial subsalt velocity model with a classic velocity trend, i.e., normal compaction trend (Figure 3a).

b) Produce RTM 3D angle gathers and image of the synthetic 'field' records with the initial model (Figure 3b). Stronger BOS amplitudes can be noticed in the overpressure lower velocity zone. Extract the BOS amplitude from the RTM image (Figure 3b).

c) Perform two-way wave equation forward modeling with the initial model. Migrate with RTM using the same initial model (Figure 3c). Extract the BOS amplitude from the image and use it to determine the transmission and illumination factor ***I*** at BOS in Equation 2**.**

d) Invert the salt exit velocity from the BOS amplitude measured in step b), compensated with transmission and illumination factor ***I*** obtained from step c). The reflectivity inversion method clearly predicts the lower salt exit velocity, and the prediction error is within 4% (Figure 3e).

e) Use the predicted salt exit velocity to constrain the tomography with high fidelity RTM 3D angle gathers (Figure 3e). RTM 3D angle gathers have less artifacts than 2D ADCIGs. Run tomography by ray tracing to the BOS to improve inversion stability and accuracy (Xu et al., 2010).

f) The resulting subsalt model (Figure 3f) is used for RTM of the synthetic 'field' data. Figure 4 shows the RTM images obtained using the initial velocity model, as well as the derived subsalt model. The inverted velocity not only gives better positioning of subsalt events, but also restores the continuity and amplitudes of subsalt reflectors.

Wide Azimuth Field Data

Encouraged by the 2D synthetic results, we applied the method to a 750 sq km marine WAZ dataset in the Green Canyon area, Gulf of Mexico. Figure 5a shows spatial distribution of salt exit velocity and indicates three likely highly over-pressured zones, providing valuable information for drilling. The calculated salt exit velocity matches the check shot velocity very well (Figure 5c). The resulting subsalt model improves the subsalt image (Figure 6).

Conclusions

Because of the high drilling cost in the deepwater Gulf of Mexico, pre-drill pore-pressure predictions are vitally important in deepwater areas with extreme depth and drilling window conditions. Reflectivity inversion from true-amplitude RTM, integrated with high-resolution tomography of RTM 3D angle gathers can successfully derive the salt exit velocity for 2D synthetic data, as well as 3D WAZ field data. Consequently, the calculated salt exit velocity results in more coherent subsalt images and provides a good starting point for further velocity updates.

Acknowledgments

We would like to thank Monica Thomas for her work in the field data example. We are grateful to Sam Gray, Kristin Johnston, and Shannon Strine for reviewing the paper.

References

Brown, M. and J.H. Higginbotham, 2009, Sub-salt overpressure detection before drilling using wave equation migration technologies, SEG Expanded Abstracts **28**, 1800-1804.

Hawkins, K., A. Ratcliffe, G. Roberts and D. Went, 2004, High resolution pore-pressure prediction from AVO derived velocities; a North Sea case study, SEG Expanded Abstracts, **23**

Ji, S., T. Huang, K. Fu and Z. X. Li, 2010, Dirty Salt Velocity Inversion: The Road to a Clearer Subsalt Image. SEG Expanded Abstracts **29**, 4103-4107.

Xu, S., Y. Zhang and B. Tang, 2010, 3D common image gathers from Reverse time migration. SEG Expanded Abstracts **29**, 3257-3262.

Zhang, Y. and J. Sun, 2009, Practical issues of reverse time migration: true-amplitude gathers, noise removal and harmonic-source encoding. First Break, **27**, no. 1, 53–59.

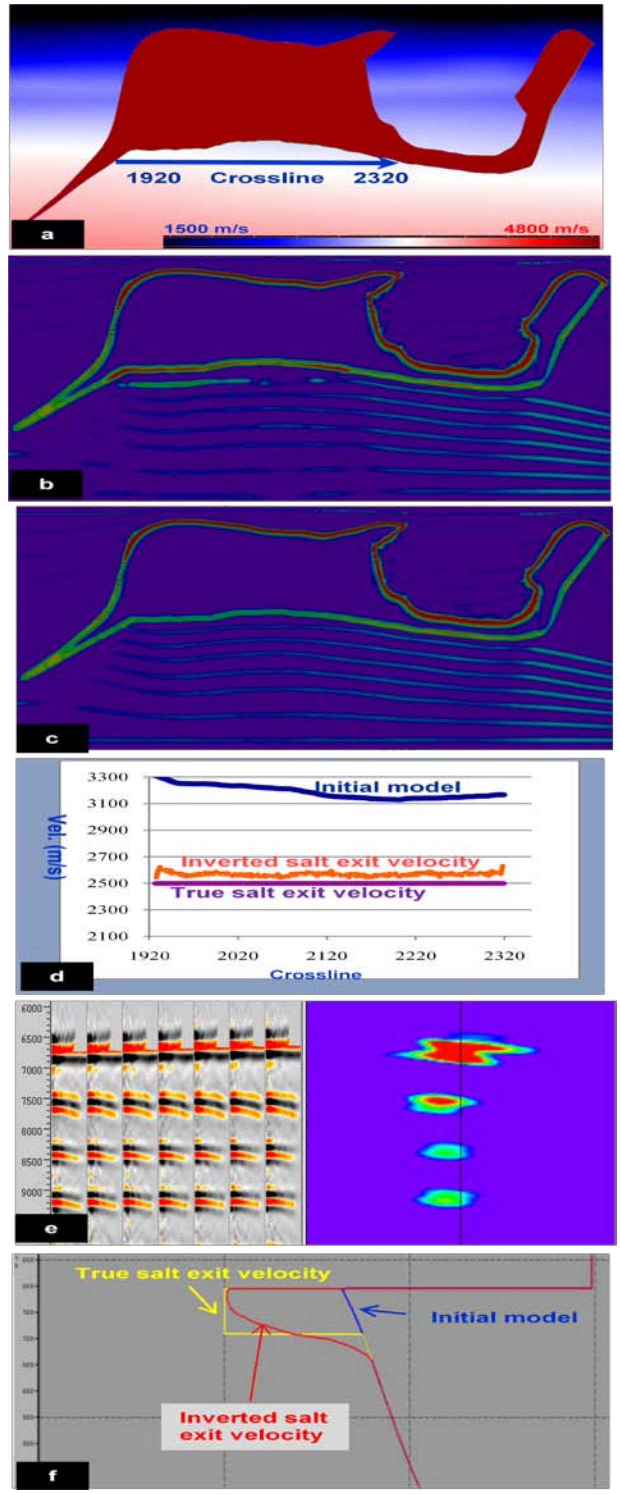

Figure 3: a) Initial model with normal subsalt velocity trend; b) Amplitude extracted from RTM with initial model using synthetic 'field' data; c) Amplitude extracted from RTM with initial model using synthetic data generated from the same model. This is used to determine the transmission and illumination factor; d) Inverted salt exit velocity is within 4% error; e) Angle gathers and semblance in subsalt at cdp location indicated by yellow arrow in b); f) Inverted velocity away from BOS from subsalt tomography with RTM gathers.

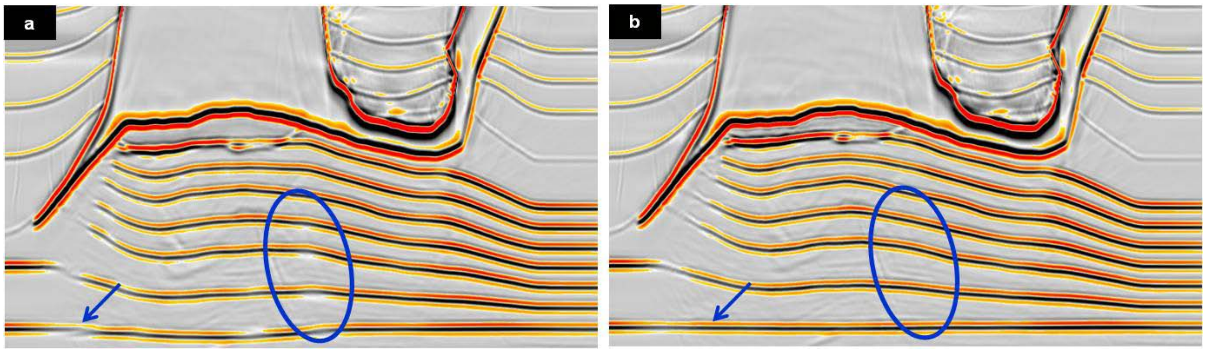

Figure 4: a) RTM with the initial model; b) RTM with the inverted subsalt velocity.

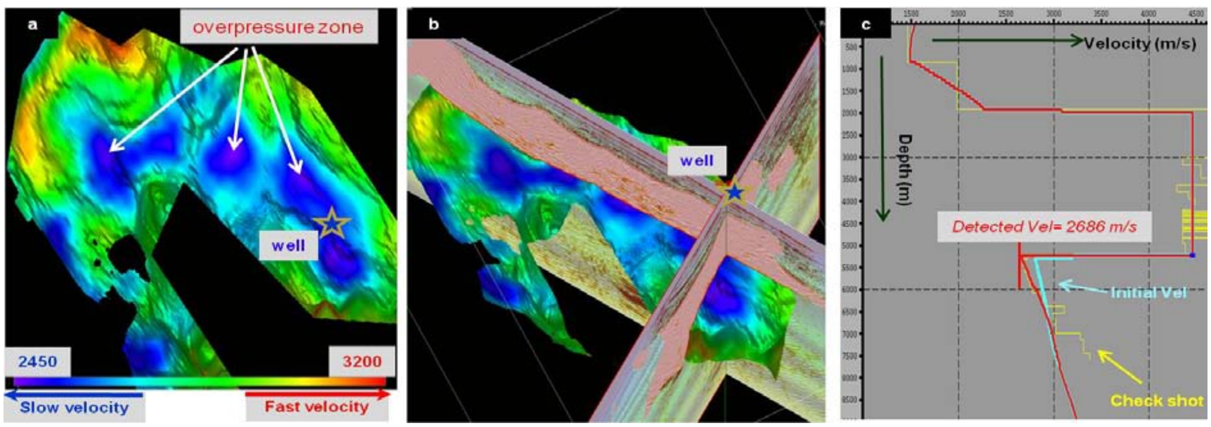

Figure *5*: a) Inverted salt exit velocity at BOS**;** b)3D view of salt exit velocity and seismic image; c)Velocity profiles of initial velocity (cyan line), salt exit velocity (red line), and check shot (yellow line).

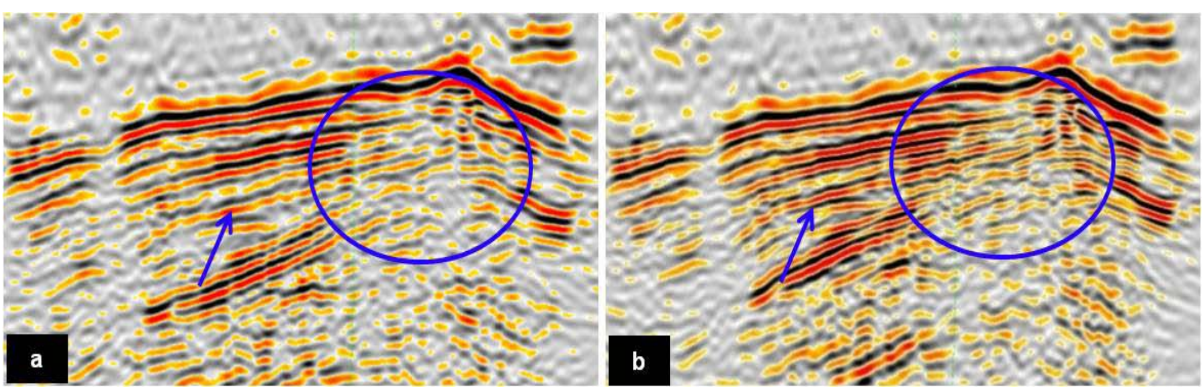

Figure 6: RTM image near the well: a) with initial model; b) with the derived salt exit model.